Available online at www.sciencedirect.com

ScienceDirect

Underground Space 2 (2017) 149–167

www.elsevier.com/locate/undsp

# Long-term tunnel behaviour and ground movements after tunnelling in clayey soils

Kenichi Soga [a], Richard George Laver [b], Zili Li [c,*]

[a] Department of Civil and Environmental Engineering, University of California, Berkeley, Berkeley, CA 94720-1710, USA
[b] Golder Associates (Hong Kong) Limited, 17/F, No. 88 Gloucester Road, Wan Chai, Hong Kong
[c] Civil & Environmental Engineering Building, University College Cork, College Road, Cork, Ireland

Received 7 May 2017; received in revised form 31 July 2017; accepted 2 August 2017
Available online 5 September 2017

**Abstract**

Long term ground movements above a tunnel may continue to increase with time after tunnelling in clayey soils as the tunnelling-induced excess pore water pressures dissipate, whilst the changing earth pressure acting on the tunnel leads to further tunnel deformation during consolidation. Furthermore the tunnel itself introduces new drainage conditions; that is, depending on the drainage condition of the tunnel lining, the effective stresses around the tunnel change with time, inducing further soil consolidation. A seepage rate from low permeability clayey soil is often very small and the groundwater seeping into the tunnel can evaporate quickly. Although a tunnel may look impermeable because the surface looks dry, it is possible that the tunnel drainage conditions are actually permeable. This paper summarises the investigation of soil-tunnel consolidation interaction, particularly focusing on ground surface movements and tunnel lining deformation in the interest of engineering concerns. Analysis results show that tunnel lining permittivity relative to the permeability of the surrounding ground plays an important role on both long-term ground movements as well as tunnel lining behaviour. The findings published in literature are reviewed step by step starting from a single tunnel, twin tunnels to complex cross passage structures. The mechanisms of tunnelling-induced soil consolidation for these structures are identified and, where applicable, possible engineering methodologies to assess the magnitude of long-term ground surface settlements and tunnel lining loads are proposed.


*Keywords:* Radial seepage flow; Long-term horizontal strain; Twin tunnel interaction; Cross passage deformation; Settlement evaluation method

**Contents**



* Corresponding author.
*E-mail addresses:* soga@berkeley.edu (K. Soga), richlaver@cantab.net (R.G. Laver), zili.li@ucc.ie (Z. Li).
Peer review under responsibility of Tongji University and Tongji University Press.

http://dx.doi.org/10.1016/j.undsp.2017.08.001

**Nomenclature**

| | |
|---|---|
| $a_{hd}$ | offset of maximum horizontal displacement from tunnel centreline |
| $A_{RS}$ | coefficient in relative settlement equation |
| $B_{RS}$ | coefficient in relative settlement equation |
| $C$ | cover of soil above tunnel crown |
| $C_{clay}$ | Cover of clay above tunnel crown |
| $D$ | tunnel diameter, or soil parameter controlling non-linearity during isotropic loading and unloading |
| $DS$ | dimensionless surface settlement with respect to extremes of permeability behaviour |
| $E'_d$ | representative drained soil modulus for consolidating zone |
| $E$ | Young's modulus |
| $e$ | void ratio |
| $H_c$ | horizontal displacement experienced during consolidation |
| $H_{c\ max}$ | maximum consolidation horizontal surface displacement in a transverse distribution |
| $k_s$ | representative isotropic soil permeability; $\sqrt{(k_h k_v)}$ if anisotropic |
| $k_h$, $k_v$ | soil permeabilities: horizontal and vertical |
| $K_L$ | parameter for width of consolidation settlement trough |
| $K_t$ | lining seepage coefficient |
| $k_t$ | lining permeability |
| $L_c$ | tunnel axis depth below water table |
| $NH_{c\ max}$ | non-dimensional maximum consolidation horizontal surface displacement |
| $NH_{c\ max\ (ss)}$ | $NH_{c\ max}$ at steady-state |
| $NS_{c\ max}$ | non-dimensional maximum consolidation surface settlement |
| $NS_{c\ max\ (ss)}$ | $NS_{c\ max}$ at steady-state |
| $RP$ | relative soil-lining permeability |
| $RS_{c\ max}$ | relative settlement as proportion of steady-state settlement |
| $S_c$ | settlement experienced during consolidation |
| $S_{c\ max}$ | maximum consolidation settlement in a transverse trough |
| $S_{c\ max\ (ss)}$ | $S_{c\ max}$ at steady-state |
| $t$ | consolidation time, or lining thickness |
| $T_v$ | dimensionless time factor for consolidation |
| $V_L$ | volume loss as fraction of tunnel cross-sectional area |
| $x$ | transverse distance from tunnel centreline |
| $z_0$ | tunnel axis depth below ground level |
| $\alpha$ | parameter for modified Gaussian curve |
| $\gamma_w$ | bulk unit weight of water |
| $\varepsilon^c_{c\ max}$, $\varepsilon^f_{c\ max}$ | peak consolidation horizontal strain: at centreline and in far-field |
| $\varepsilon^c_{c\ max\ (ss)}$, $\varepsilon^f_{c\ max\ (ss)}$ | $\varepsilon^c_{c\ max}$ and $\varepsilon^f_{c\ max}$ at steady-state |
| $\mu$ | parameter for width of consolidation settlement trough |



## Introduction

In clayey soils, ground movements above a tunnel can continue to build up following construction whilst the tunnel develops a further deformation as the soil consolidates (e.g. Bowers, Hiller, & New, 1996; Harris, 2002; Laver, Soga, Wright, & Jefferis, 2013; Nyren, 1998; O'Reilly, Mair, & Alderman, 1991; Peck, 1969; Shirlaw, 1995). The increasing consolidation settlement may induce surface building damages, for example, as reported by Harris (2002), above the Jubilee Line Extension tunnels in London, whilst long-term tunnel deformation may lead to cracks, water infiltration and differential displacements at risk of derailment for tunnel safety (Shen, Wu, Cui, & Yin, 2014).

Shirlaw (1995) stated that long-term ground surface displacements during consolidation can account for 30–90% of the total settlement. The continuing ground settlement with time is caused by consolidation of the surrounding clay by the dissipation of excess pore pressures generated during tunnel excavation and decreasing pore water pressures and hence increasing effective stress around the

tunnel by seepage. Large differential settlement can occur at cross passage and ramp sections, which are usually more permeable than main tunnel sections (Shen et al., 2014). For example, significant cumulative differential tunnel settlements were observed in Shanghai Metro Line No. 1 over 12.5 years after construction (Ng, Liu, & Li, 2013), and such differential settlements have led to serious longitudinal deformation and groundwater infiltration for the safety of tunnel linings (I.T.A. Working Group No. 2 (ITA), 2000; Shen et al., 2014).

The magnitude and rate of consolidation-induced settlement are related to the following (e.g. Martinez, Schroeder, & Potts, 2014; Shin, Potts, & Zdravkovic, 2002; Wongsaroj, Soga, & Mair, 2007; Wongsaroj, Soga, & Mair, 2013).

- permittivity (permeability divided by thickness) of lining, which also considers drainage along the joints,
- pore water pressure conditions around the tunnel (before and after tunnelling, throughout its life time),
- permeability and compressibility of clay and their anisotropic characteristics,
- ground conditions such as clay's thickness and drainage conditions, and
- The magnitude of excess pore pressures that develop during construction.

To predict consolidation induced long-term ground displacements, Wu, Xu, Shen, and Chai (2011) and Zhang, Liu, and Huang (2013) conducted soil-fluid coupled FE analysis and built a linear relationship between ground settlement and the water volume leaked into tunnel. However, in practice, it is difficult to quantify the amount of water leakage rate into a tunnel in clayey soils. That is, the small amount of water seeping into the tunnel is likely to evaporate once it is exposed to air, whereas large measurable amount of water seeping is seldom permitted in the interest of tunnel safety. Wang, Wong, Li, and Qiao (2012) conducted a finite element analysis of long-term surface settlement above a shallow tunnel in soft ground. They examined the influence of soil creep, consolidation and lining permeability, and particularly pointed out that the creep behaviour of soft clay can play an important role on the long-term settlements. However, in very low permeability soil, consolidation settlement around a tunnel can take a few decades or more and hence it will be difficult to separate any time dependent movement into the consolidation-induced one and the creep-induced one.

As it is difficult to quantify the permittivity value of tunnel lining (due to complicated water ingress at the segmental joints), a monitoring based prediction of long-term consolidation induced settlement has been proposed (Laver, Li, & Soga, 2016). The work is originally based on Wongsaroj et al. (2007), Wongsaroj et al. (2013), who devised a method to predict the long-term surface settlements for a single tunnel constructed in London Clay based on the results of a finite-element parametric study and field data interpretation. The work indicated that the consolidation surface settlements can be fitted well by a modified Gaussian curve, and the settlements build up with time at a logarithmically decreasing rate. They used the field data from the St James Park site as part of the Jubillee line extension (Nyren, 1998) and at the Heathrow Express site (Bowers et al., 1996). Hover, Psomas, and Eddie (2015) recently reported the field measurements above Whitechapel station tunnel in London, in which the rate of consolidation settlement agreed with the logarithmic trend. The measured settlements one year after construction were used to predict further settlements at 10 and 120 years when a steady-state condition is reached.

For tunnel structures themselves, the development of earth pressure around the tunnel during soil consolidation can induce further structural deformation. Addenbrooke (1996) and Tube Lines (2007) report that tunnel lining in London Underground usually sustains about 60% full overburden at the stead-state condition when the soil consolidation completes and the tunnel often squats in the long term. Similar deformation mode was also observed in the majority of the metro tunnels in Shanghai (Shen et al., 2014), where the most excess pore pressure generated by tunnelling fully dissipated in 2.5 months after construction as reported by Lee, Ji, Shen, Liu, and Bai (1999) in Shanghai metro tunnel Line 2. In particular, the largest tunnel ovalisation and diametrical distortion appeared in the rings adjacent to the cross passage (Shen et al., 2014). Likewise, the engineering conditions of old cross passages between adjacent cast-iron tunnels in London Underground were also founded by found to be critical by recent assessment (Wright, 2010). Li, Soga, and Wright (2015) made an attempt to investigate the twin-tunnel consolidation interaction behaviour and then cast-iron cross passages in London clay. They examined the influence of cross passage and relative soil-lining permeability on ground response as well as tunnel lining behaviour, and found that the soil load profile applied to the tunnel linings was very much influenced by the presence of cross passage.

This paper summarises the findings of selected studies on long-term ground movements and tunnel lining behaviour after tunnelling in clayey soil. The tunnel drainage and soil consolidation mechanism is described first, which is followed by the definitions of dimensionless parameters to make different tunnelling conditions comparable. The knowledge of soil-tunnel interaction mechanisms helps us to understand the long-term ground surface movements and tunnel structural performance. The paper describes the mechanisms deduced from the numerical simulations and limited field observations of a simple single tunnel case to more complicated cases of twin-tunnel and tunnel cross passage cases (Li, Soga, & Wright, 2016; Li et al., 2015).

## Tunnel drainage mechanism

Some earlier research demonstrates that tunnel may act as new drainage boundaries in low-permeability clayey

soils based upon the field measurements of pore pressures around tunnels (e.g. Palmer & Belshaw 1980; Ward & Thomas 1965). Ingress of water into the Jubilee Line Extension (JLE) tunnels were reported by Nyren (1998) and Harris (2002), confirming that the tunnels were acting as drains in this case as illustrated in Fig. 1.

As the first dedicated attempt, Wongsaroj (2005) and Wonsaroj et al. (2013) devised a method to predict long-term surface settlements for a single tunnel constructed in London Clay. Results of their finite-element parametric study show that the tunnelling-induced long-term soil consolidation mainly depends on the drainage conditions of the tunnel relative to the surrounding soil; that is, the fully drained tunnel conditions relative to low permeability soil induce large settlement because of increased effective stress (i.e. by the decrease in pore water pressure at the tunnel boundary) in the soil around the tunnel. In the impermeable lining case, on the other hand, there is no seepage-induced consolidation and therefore less consolidation-induced settlement is observed. For such case in overconsolidated clays, consolidation ground heaving may be observed due to time-dependent swelling, which is associated with the dissipation of negative excess pore pressures that develop when the ground is sheared during the construction of the tunnel (Wongsaroj et al., 2013).

Wongsaroj (2005) and Wongsaroj et al. (2013) simplified the groundwater seepage into tunnel as one-dimensional flow downward only from the tunnel crown but ignored the water flowing from the rest of the tunnel boundary (Fig. 1(1)). Laver (2010) and Laver et al. (2016) improved the evaluation method of Wongsaroj et al. (2013) by adopting a more realistic water flow pattern into the tunnel. In the new evaluation method, the hydraulic field around the tunnel is considered as a radial flow model (see Fig. 1 (2)), which lays the basis of the definition of a non-dimensional parameter for long-term consolidation vertical surface settlement ($NS_{c\ \max}$).

$$NS_{c\ \max} = \frac{E'_d}{5DL_c\gamma_w} S_{c\ \max} \tag{1}$$

where $D$ is the tunnel diameter. $E'_d$ is the equivalent 1D drained modulus taken at tunnel axis depth in the middle

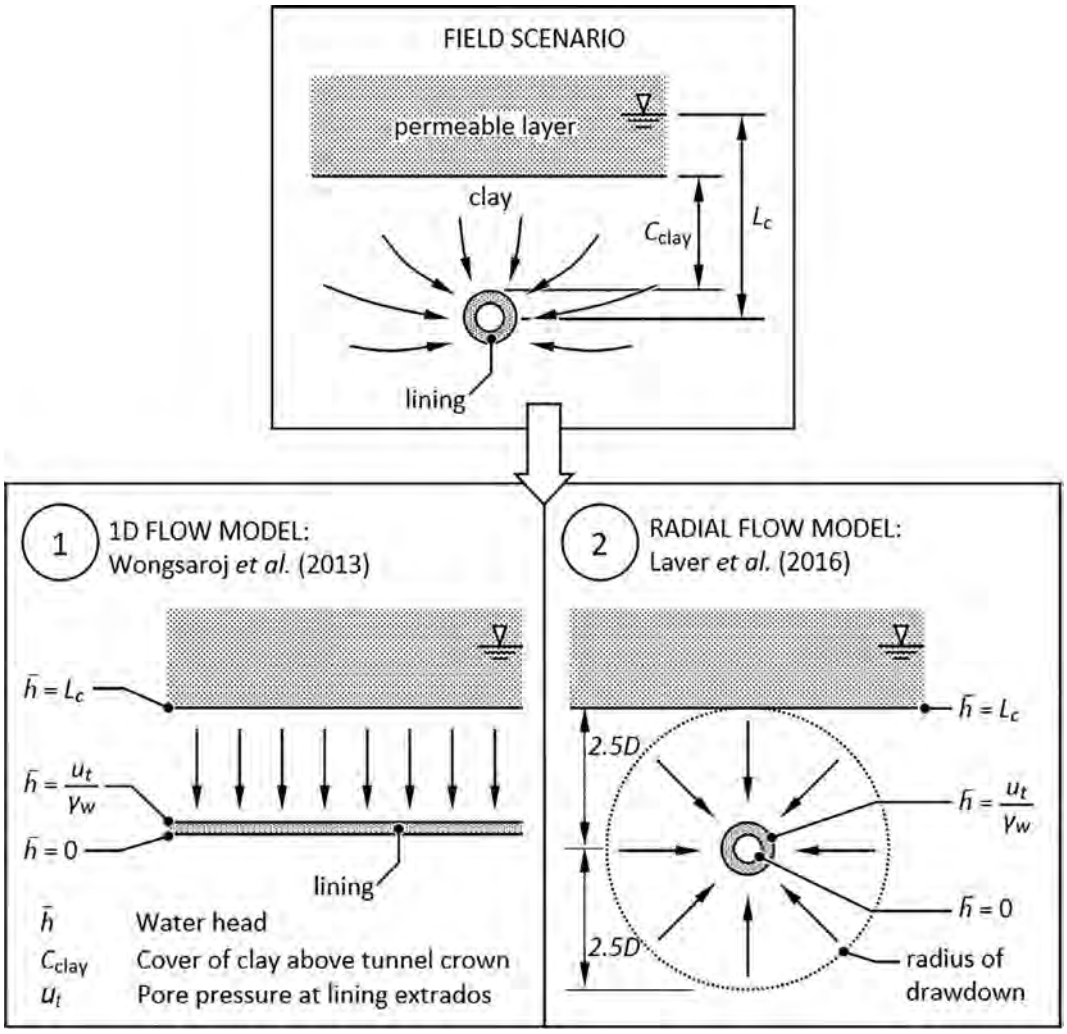


Fig. 1. Mathematical models for deriving relative soil-lining permeability (Laver et al., 2016).

of the consolidating layer correspondingly, $L_c$ is the tunnel axis depth below the water table, $\gamma_w$ is the bulk unit weight of water, $S_{c\ max}$ is the vertical surface settlement at the centreline of the tunnel by consolidation only. The thickness of the consolidating layer is taken as the diameter of the consolidating zone $5D$, which means between $\pm 2.5D$ from axis depth (Fig. 1(2)). The FE simulation results of Laver et al. (2016) show that 70–90% of consolidation occurs within this region for the fully permeable lining case. Similar observation was made in the field for London Clay (Glossop & O'Reilly, 1982; Harris, 2002; Nyren, 1998), where, for instance, the measured subsurface consolidation settlement 12 m above the westbound tunnel at St James's Park (i.e. +2.5 D from axis depth) is 6.7 mm, which is already 77% of the consolidation settlement (8.7 mm) near the ground surface (Nyren, 1998). It is noted here that the total settlement will be the summation of the short term settlement and the consolidation settlement. The latter is considered in this paper.

If the radial flow pattern into a tunnel is considered, the following relative soil-lining permeability $RP$ is derived (Laver et al., 2016).

$$RP = \frac{DK_t\gamma_w}{2k_s}\ln\left(\frac{2C_{\text{clay}}}{D}+1\right) \tag{2}$$

where $K_t$ is the lining seepage coefficient ($k_t/\gamma_w t$), $k_t$ is the lining permeability, $t$ is the lining thickness, $C_{clay}$ is the clay cover thickness, $k_s$ is the average equivalent soil permeability ($=\sqrt{k_h k_v}$), $k_v$ and $k_h$ are the vertical and horizontal soil permeability, respectively. The others are defined earlier. By increasing the lining seepage coefficient $K_t$ (or permittivity) the tunnel becomes more permeable in comparison to the surrounding ground (i.e. bigger $RP$). Fig. 2 demonstrates that the tunnel is considered as impermeable if $RP < 10^{-1}$, whereas the tunnel becomes fully permeable if $RP > 10^{2}$ (Laver et al., 2016).

The abovementioned non-dimensional soil-tunnel parameters (e.g. non-dimensional displacement ($NS_{c\ max}$) and relative soil-lining permeability index ($RP$)) make different tunnelling conditions comparable when evaluating long-term ground movements as well as tunnel behaviour, which are described in the following sections.

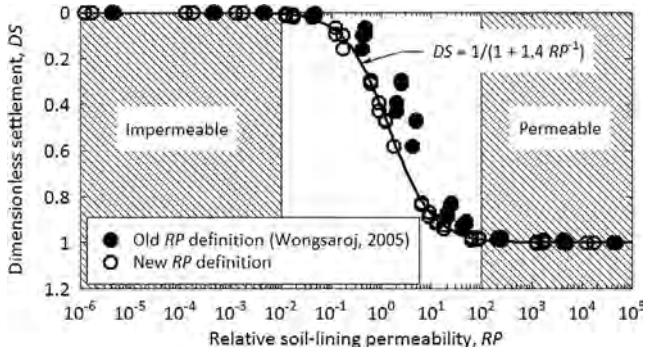


Fig. 2. Dimensionless settlements ($DS$) for relative soil-lining permeability (Laver et al., 2016).

## Single tunnel

### *Ground movements*

#### *Vertical movements*

Martos (1958) and Peck (1969) and many other authors demonstrated that the short-term transverse settlement trough shape induced by tunnelling in greenfield conditions could be expressed by the following Gaussian curve:

$$\mathrm{S}(x) = S_{\max}\exp\left(\frac{-x^2}{2i^2}\right) \tag{3}$$

where $S$ is the ground settlement, $S_{max}$ is the maximum settlement on tunnel centreline, $x$ is the horizontal distance from tunnel centreline, i is the horizontal distance of inflexion point from tunnel centreline.

Such normal Gaussian curve is often used to characterise the ground deformation immediately after tunnel construction. However, it has difficulty in fitting the long-term surface settlement, which usually becomes wider and deeper during consolidation (Wongsaroj et al., 2013). By incorporating an additional parameter, Vorster, Klar, Soga, and Mair (2005) proposed a modified Gaussian curve to fit the observed soil settlement in his work:

$$\mathrm{S} = \frac{\mathrm{n}}{(n-1)+\exp[\mu(x/i)^2]}S_{\max} \tag{4}$$

$$n = \exp(\mu)\times\left(\frac{2\mu-1}{2\mu+1}\right)+1 \tag{5}$$

where $n$ is the shape function parameter controlling the width of the profile, and $\mu$ is the parameter to ensure that $i$ remains the distance from the tunnel centreline to the inflection. Eq. (4) is the same as the normal Gaussian curve when $n = 1$, which corresponds to $\mu = 0.5$. For a given value of $i$, if $\mu < 0.5$, the modified Gaussian curve predicts a wider settlement trough than the normal curve. On the contrary, if $\mu > 0.5$, the modified curve becomes narrower than the normal one.

Wongsaroj et al. (2013) and Laver et al. (2016) adopted the modified Gaussian curve (Eq. (4)) to fit the measured long-term ground settlement at two historical cases of tunnelling in London clay as shown in Fig. 3. It is found that the consolidation settlement profiles are wider than those for the short term with the decreasing values of $\mu$ from 0.5 (i.e. normal Gaussian curve) to approximately 0.1 during soil consolidation, whereas the locations of the inflection point did not change much; The values of $i/z_0$ (where $z_0$ is the tunnel axis depth) for the three cases presented in the figure are between 0.35 and 0.45 for the short term immediately after excavation, and then between 0.31 and 0.39 after some consolidation.

Mair (2008) conducted finite element analysis to evaluate the influence of soil permeability anisotropy on the long-term ground surface settlement. The numerical results also show that the consolidation-induced settlement trough is wider than the short-term settlement due to tunnel

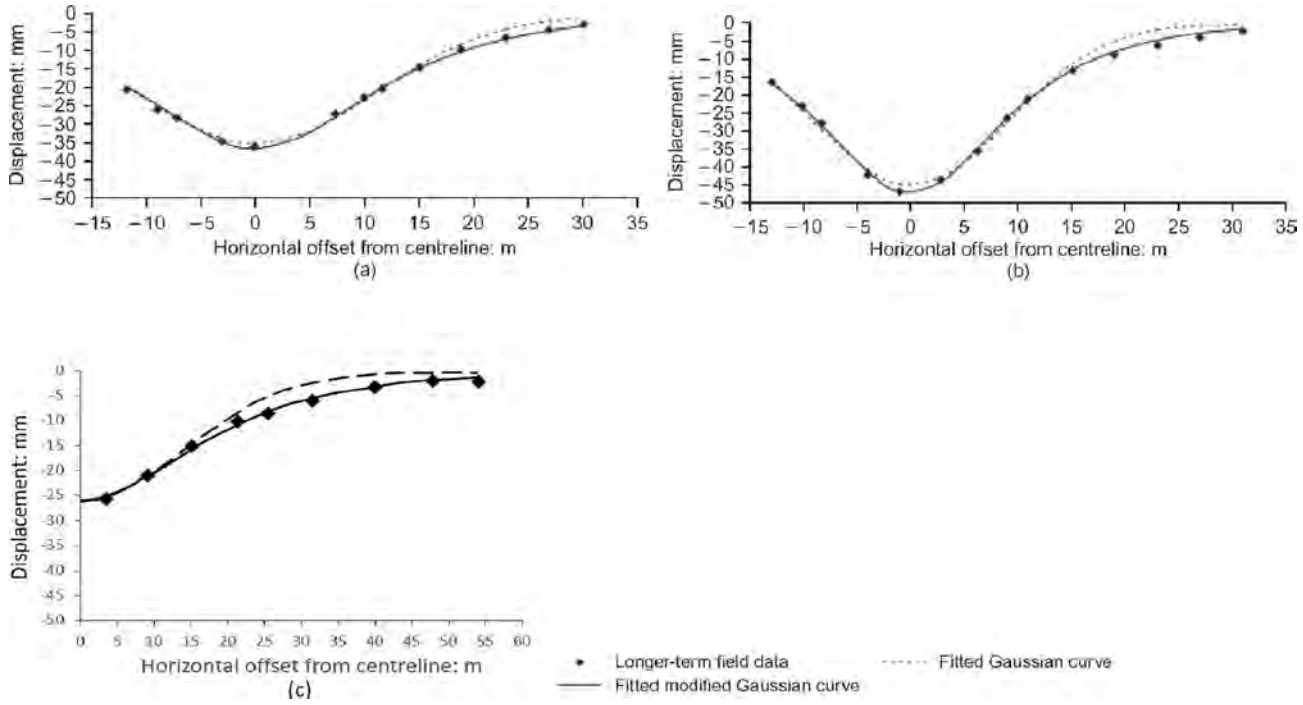


Fig. 3. Discrepancies between total surface settlement profiles after excavation, and Gaussian-type curves. Heathrow Express trial tunnel, field data 3.3 years after excavation (Bowers et al.,1996): (a) Type 1 and (b) Type 2. (c) St James's Park westbound tunnel, field data 255 days after excavation (Nyren, 1998; Wongsaroj et al., 2013).

construction, while the consolidation-induced settlement trough of the anisotropic case is wider than for the isotropic permeability case, if the soil surrounding the tunnel is more permeable in the horizontal direction than the vertical one. A more comprehensive study on this aspect was made by Wongsaroj et al. (2013). Fig. 4 shows the influence of soil–lining relative permeability and soil permeability anisotropy on long-term consolidation trough width parameters; ($\mu$ and $K_L = i/z_0$). According to the modified Gaussian curve in Eq. (1), a decrease in $\mu$ leads to a wider settlement trough, whereas an increase in $K_L$ moves the inflection point further away from the tunnel centreline. As the soil permeability anisotropy $k_h/k_v$ increases from 1 to 10, the decreasing $\mu$ and increasing $K_L$ results in a wider consolidation settlement trough. Such effect of permeability anisotropy is negligible for impermeable tunnel (e.g. $RP < 10^{-1}$) but significant for permeable cases (e.g. $RP > 10^{2}$).

The actual ground displacement at any particular consolidation time of interest is given by scaling the steady-state displacements using a relative displacement $RS_{c\ \max}$ defined proposed by Wongsaroj et al. (2013) as follows:

$$S_{c\ \max} = RS_{c\ \max} S_{c\ \max(ss)} \tag{6}$$

where $RS_{c\ \max}$ is related to the dimensionless time factor $T_v$, depending on the magnitude of the soil permeability and drainage distance (Wongsaroj et al., 2013):

$$T_v = \frac{E'_d k_s}{C^2_{clay}\gamma_w} t \tag{7}$$

where $t$ is consolidation time after construction, while other parameters are mentioned earlier. The dimensionless time factor $T_v$ is consequently adopted with the following relationship proposed by Laver et al. (2016) to account for lining permeability and tunnel geometry:

$$RS_{c\ \max} = 1 - \frac{2}{3}\exp\left[\ln\left(\frac{3}{2}\right) - 3A_{RS}T_v^{B_{RS}}\right] \tag{8}$$

where $A_{RS}$ and $B_{RS}$ are functions of $C/D$ and $RP$ using curve fitting to finite element parametric simulations, whilst the derivation of the equation can be found in Laver (2010).

*Horizontal movements*

For the horizontal displacement distribution, Laver et al. (2016) suggested a two-parameter curve as follows:

$$H_c = \frac{3a_{hd}^2 H_{c\ \max} x}{|x|^3 + 2a_{hd}^3} \tag{9}$$

where $x$ is the distance from the centreline, $a_{hd}$ is the offset from the centreline of the maximum horizontal consolidation-induced displacement $H_{c\ \max}$, and more details can be found in Fig. A.1 of the Appendix.

Of particular interest is the peak horizontal strains (i.e. peak compressive strain $\varepsilon^c{}_{\max}$ at the tunnel centerline and peak tensile strain $\varepsilon^f{}_{\max}$ away from the tunnel), which is a concern in evaluating tunnelling-induced building damage (Burland, 1995). For the long-term horizontal movements, past studies found that the build-up of horizontal displace-

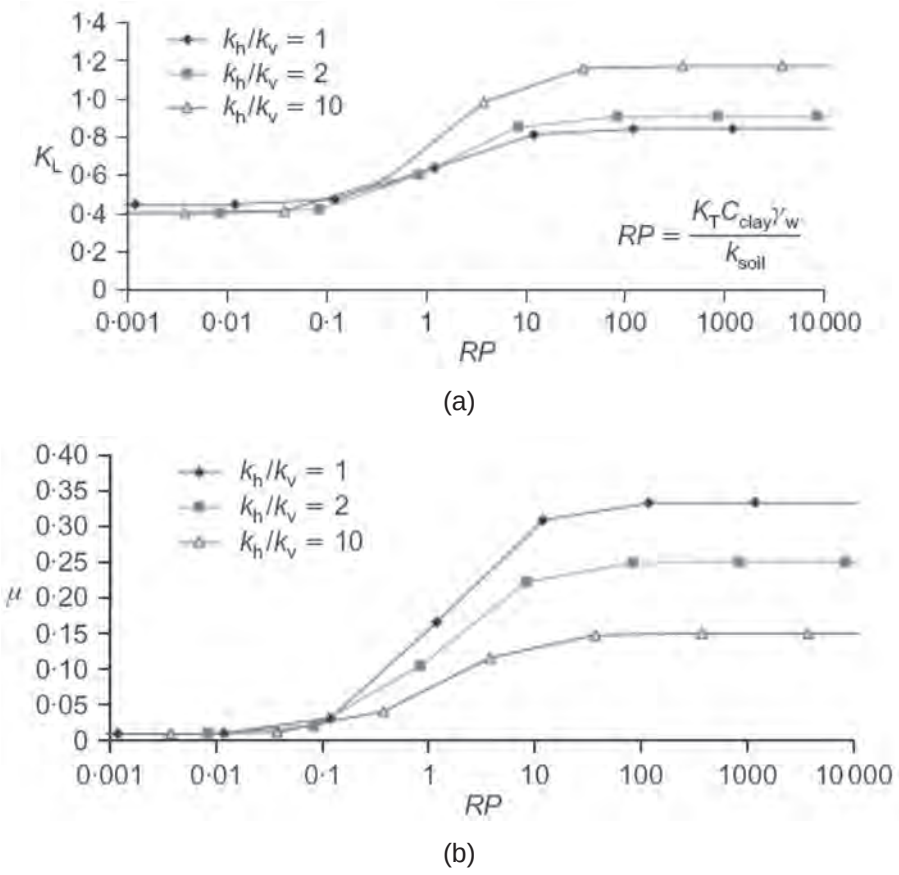


Fig. 4. Influence of soil–lining relative permeability and soil permeability anisotropy on long-term consolidation settlement trough width parameters (Wongsaroj et al., 2013).

ments and strains during consolidation are much smaller than those induced by short-term tunnel excavation, suggesting that further building damage is unlikely to occur (e.g. Bowers et al., 1996; O'Reilly et al.,1991). Laver et al. (2016) recently reported some new findings on consolidation horizontal strains from the results of soil-fluid coupled finite element analysis investigating the long-term ground movements above the following two tunnel cases: (1) St James's Park case (Nyren, 1998) and (2) Heathrow Express trial tunnel case (Bowers et al., 1996).

Fig. 5a shows that the development of computed maximum consolidation-induced horizontal strains with time at the St James's Park case. Although the computed maximum tensile and compressive consolidation-induced strains induced by consolidation are not considerable at $t = 235$ days (the end of field monitoring), the prediction based on the model by Laver et al. (2016) continue to increases with time up to $1.72 \times 10^{-4}$ and $-7.74 \times 10^{-4}$, respectively, at $t = 10$ years, which can be similar in magnitude to the short-term tunnelling induced movements reported by Nyren (1998), where the short-term tensile and compressive strains induced by tunnel excavation were $5 \times 10^{-4}$, and $-1.0 \times 10^{-3}$, respectively as shown by circles in Fig. 5a.

As another example, the development of estimated consolidation-induced horizontal strains with time for the Heathrow Express case is given in Fig. 5b. The estimated maximum tensile and compressive consolidation-induced strains at $t = 1220$ days after excavation are $1.58 \times 10^{-4}$ and $-6.70 \times 10^{-4}$, respectively; they are 31.6–55.8% of the measured short-term maximum strains generated by tunnel excavation (i.e. immediate tensile strain $= 5.0 \times 10^{-4}$ and immediate compressive strain $= -12.0 \times 10^{-4}$). These values generally agree with the field measurements that no considerable strain development was observed at $t = 1220$ days after tunnel construction (Bowers et al., 1996). However, the predicted consolidation induced strains increase up to $2.68 \times 10^{-4}$ in tension and $-11.4 \times 10^{-4}$ in compression at $t = 30$ years; these are 53.6–95.0% of the measured short-term tunnel induced strains. Hence, also in this case, the long term consolidation-induced ground movements at the steady state may become similar in magnitude to the short term ground movements immediately after tunnel construction.

### *Lining behaviour*

Many field observations concur that tunnel lining load keeps building up after tunnel excavation in clayey soil until a steady-state flow condition is reached after many years. Theoretically, an impermeable tunnel sustains more

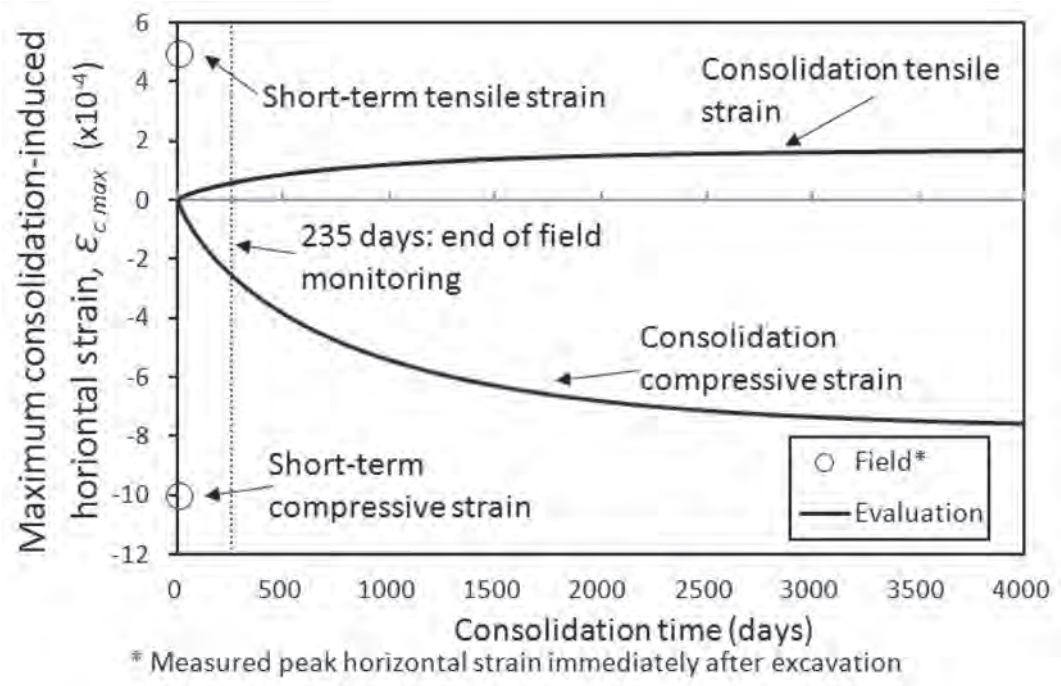


(a) St James's Park tunnel

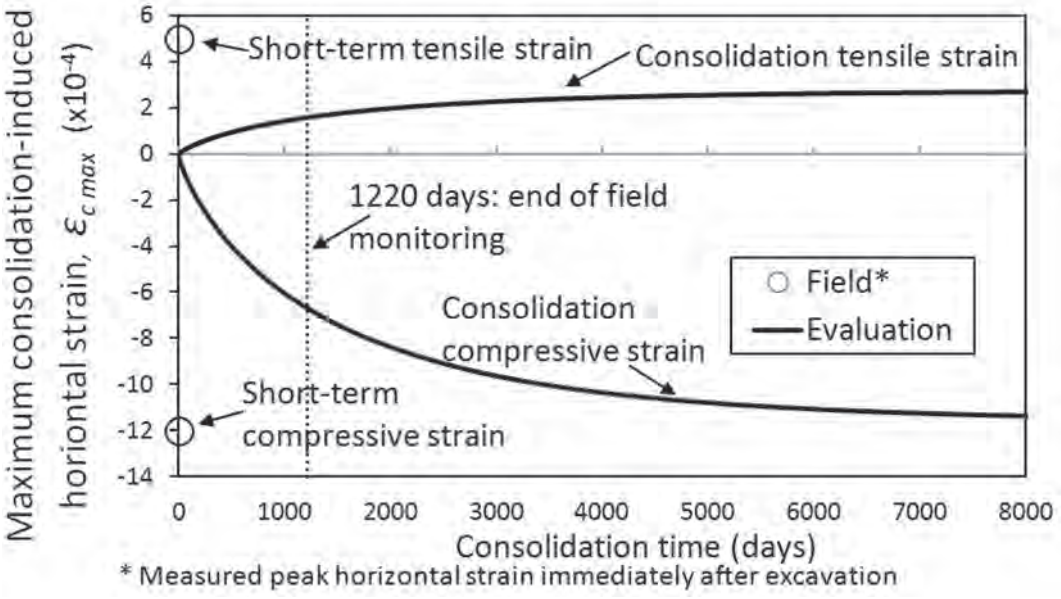


(b) Heathrow Express trial tunnels

Fig. 5. Development of computed consolidation-induced horizontal strains with time (Laver et al., 2016).

lining load than a permeable one due to the recovery of pore-water pressure in the long term (Shin et al., 2002). In fact, Mair (2008) demonstrates that the old tunnels in London Clay are almost fully-permeable in practice and act as drains. Based upon many previous efforts (Bowers et al., 1996; Peck, 1969; Ward & Thomas, 1965), Addenbrooke (1996) and Tube Lines (2007) suggest that the lining may consequently sustain about 60% full overburden at the stead-state condition, whilst the tunnel squats in the long term. Li et al. (2015) conducted a finite element analysis of old tunnels in stiff low-permeability London clay and noticed that most of the tunnel squatting builds up within 2000 days (i.e. about 5.5 years) after tunnel construction as the soil around the tunnel gradually

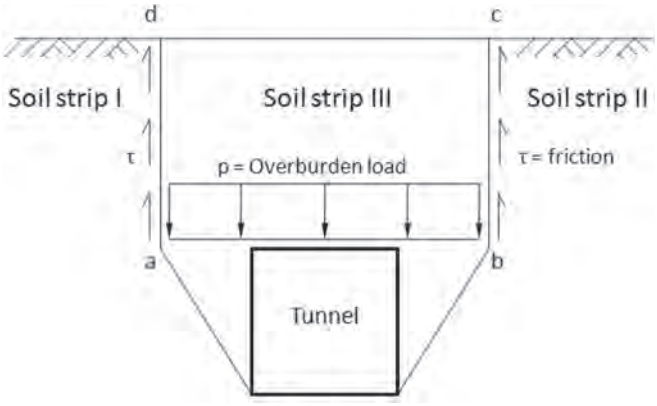


(a) The soil strip model for illustrating the soil arching effect (Terzaghi, 1943)

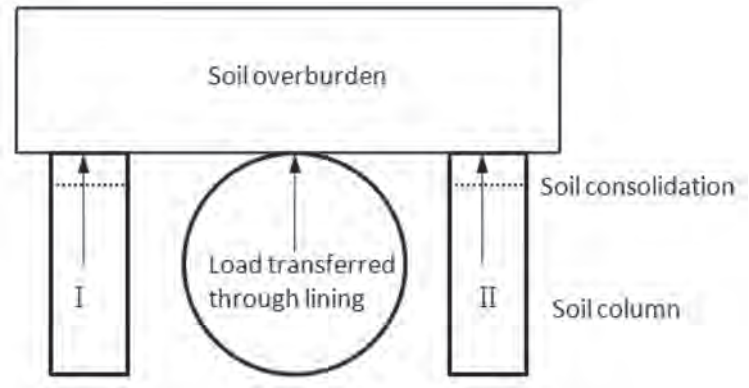


(b) Single tunnel load-analogy of three load columns (Dimmock, 2003)

Fig. 6. The effect of consolidation on tunnel lining (Li et al., 2015).

reaches a new steady-state flow condition. The time to reach steady state long-term tunnel deformation is much shorter than that of ground settlement; the latter usually continues to build up after several decades. This is because the water pressure distribution around the tunnel, which contributes to the lining load, tends to reach to the quasi-steady state condition within a few years. On the other hand, the dissipation of the water pressure drop propagates outwards from the tunnel with time, which in turn contributes to much longer time for the ground settlement away from the tunnel to finish.

To understand the soil arching effect induced by tunnel excavation in the short term before ground consolidation, Terzaghi (1943) proposed a simplified soil strip model to illustrate the load transfer above the tunnel as shown in Fig. 6a. In this figure, the sliding of the overburden soil strip III over the tunnel is resisted by the friction along the vertical sections ad & bc and consequently transferred to the adjacent soil strips I & II. In a similar manner, Dimmock (2003) proposed a load column mechanism to explain the effect of consolidation on tunnel lining as shown in Fig. 6b. In his mechanism, the overburden above the lining is sustained by the interaction between three load columns; one on either side of the tunnel (i.e. soil column I & II) and one through the tunnel lining itself. During tunnel excavation in clayed soil, the overburden first relies on the two soil columns at the sides of the tunnel. During consolidation, the soil columns shorten with time and retract support, thereby increasing the load transferred through the lining.

## Twin tunnels

### *Ground movements*

City tunnels are commonly constructed in pairs. However, there is limited study into the influence of closely-spaced tunnel interaction on ground movements during consolidation. Laver (2010) made the first dedicated attempt through soil-fluid coupled finite element analyses of twin tunnels, defining the steady-state interaction settlement $S_c^{int}$ as follows:

$$S_c^{int}(x) = S_c^{twin}(x) - (S_c^{sgl01}(x) + S_c^{sgl02}(x)) \quad (10)$$

where $S_c^{int}$ is the consolidation settlement at the steady-state condition as a result of the twin tunnel interaction, $S_c^{twin}(x)$ is the steady-state settlement at $x$ (horizontal distance from

tunnel centreline), $S_c^{sgl01}(x)$ is that after excavation of the first tunnel alone, $S_c^{sgl02}(x)$ is that after excavation of the second tunnel alone

Unlike the twin-tunnel interaction during excavation, omitting a typical rest period between excavations (e.g. 60 days) in low permeability soil causes little influence on ground displacements during consolidation (Laver, 2010). By assuming twin tunnels are excavated simultaneously, the long-term behaviour of twin side-by-sided tunnels is found to be influenced by (1) volume loss, (2) separation-to-depth ratio ($d'/z_0$), (3) cover-to-diameter ratio ($C/D_T$), which is defined as the cover of the soil above tunnel crown divided by tunnel diameter, and (4) relative soil-lining permeability (RP).

For twin-tunnel consolidation interaction, the mid-line between the tunnels, $S_{cmid}^{int}$, is considered as a critical point along the transverse surface settlement trough, which can be normalised analogously by the method described in Eq. (1):

$$NS_{cmid}^{int} = \frac{E_d'}{5D_T L_c \gamma_w} S_{cmid}^{int} \tag{11}$$

where $NS_{cmid}^{int}$ is the non-dimensional surface settlement at mid-line between the two tunnels.

By comparing the normalised settlement at the mid-line in different conditions, Laver (2010) identified three possible types of twin-tunnel interaction mechanisms as illustrated in Fig. 7:

*Mechanism A: strain field interaction*

During excavation, the change of deviatoric soil stress $q$ around the tunnel is much more significant than the mean effective stress $p'$ (Wongsaroj, 2005), whilst the shear stiffness degrades with strain (Laver, 2010). Since soil stiffness behaviour is usually non-linear, the larger soil strains induced by twin tunnel interaction during tunnel excavation and consolidation may cause more soil softening than those in superposition of two individual single tunnels. To distinguish the interaction induced at different conditions, the strain field interactions are decomposed into the following three mechanisms:

*Mechanism A - Seepage*

(i) **Mechanism Ai:** new drainage boundary - Regardless of volume loss due to excavation, the second tunnel introduces a new drainage boundary during soil consolidation and may cause additional surface settlement if the lining is permeable.

(ii) **Mechanism Aii:** excavation interaction when the lining is permeable - The soil softening generated by interaction during tunnel excavation would augment the consolidation strains of Mechanism Ai.

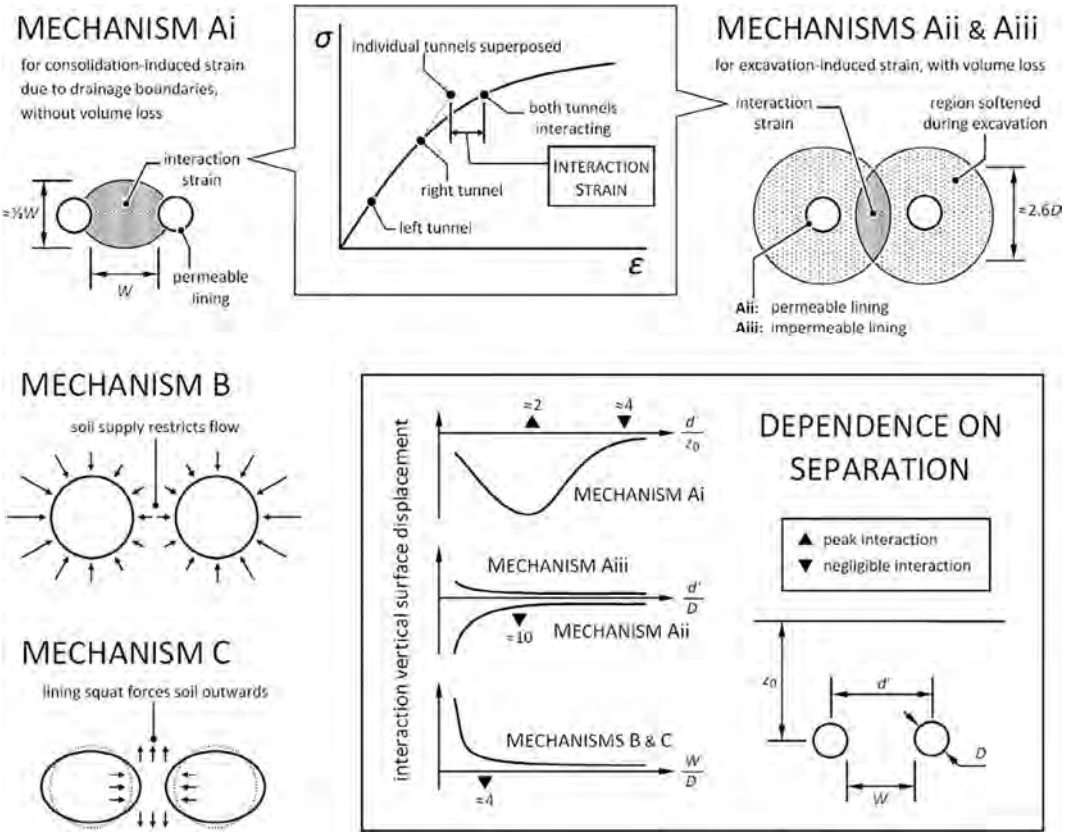


Fig. 7. Long-term twin-tunnel interaction mechanism.

(iii) **Mechanism Aiii:** excavation interaction when the lining is impermeable - The soil stiffness degrades, in a manner similar to Mechanism Aii, but allows the ground to further swell in the long term since the lining is impermeable.

*Mechanism B: Flow supply restriction*

If two tunnels are closely-spaced, the soil in between must supply water flow to both of them if the lining is permeable. However, such ability of the surrounding soil may reach a limit, as the flow supply from one side is not infinite. This reduced drainage effect restricts the ground consolidation and consequently lead to less surface settlement.

*Mechanism C: Lateral soil compression*

A fully-permeable tunnel squats as soil consolidates. If two fully-permeable tunnels are closely-spaced, their squatting during consolidation would compress the soil column in between, forcing the column to extend vertically and reducing the surface settlement.

To better understand the interaction mechanism mentioned above, Laver (2010) conducted a series of parametric studies to examine the influence of the critical factors (e.g. separation-to-depth ratio ($d'/z_0$)) on the normalised midpoint interaction settlement $NS^{int}_{cmid}$, and the computed results are illustrated in Figs. 8 and 9:

**Mechanism A:**

**Mechanism Ai:** The new drainage boundary interaction effect is dependent on separation-to-depth ratio ($d'/z_0$). If $d'/z_0>4$, such drainage interaction is negligible since the relative tunnel separation is too far away. The interaction effect builds up with the decrease of $d'/z_0$ (i.e. smaller separation or larger tunnel depth), until the two tunnels are so closely-spaced that Mechanisms B and C become active. Mechanisms B&C heave the ground and radically alter the surface settlement, but their interference in the trend for Mechanism Ai is not eliminated.

**Mechanism Aii:** The excavation interaction is more dependent upon separation-to-tunnel diameter ratio ($d'/D_T$) rather than $d'/z_0$, since the softening around the tunnel during excavation is related to the tunnel diameter. With a bigger tunnel diameter, the consolidation interaction surface settlement increases along with a wider trough region.

**Mechanism Aiii:** The interaction swelling strains generated by Mechanism Aiii for impermeable lining is significantly smaller than that of a fully-permeable lining for Mechanism Aii. Such interaction in a low level may not lead to appreciable engineering concerns.

**Mechanism B:** The flow supply restriction may only affect the ground deformation when twin-tunnels are at very close separation, since at such condition (e.g. $d'/z_0 = 0.5$) a severe reduction in drainage flow velocity is noted in the soil column between the tunnels as shown in Fig. 9.

**Mechanism C:** The effect of lateral soil compression is also likely to be influential only when the tunnels are at a small separation, since observations indicate that the horizontal strain causing the interaction reduces rapidly with distance from the tunnel.

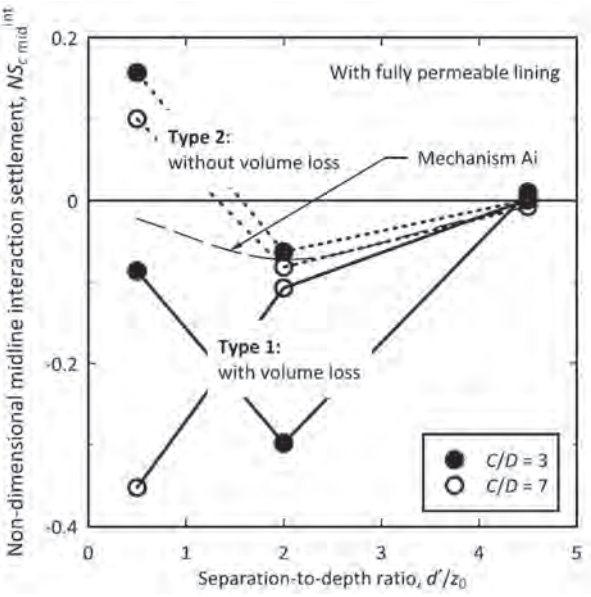


(a) For analyses with and without volume loss

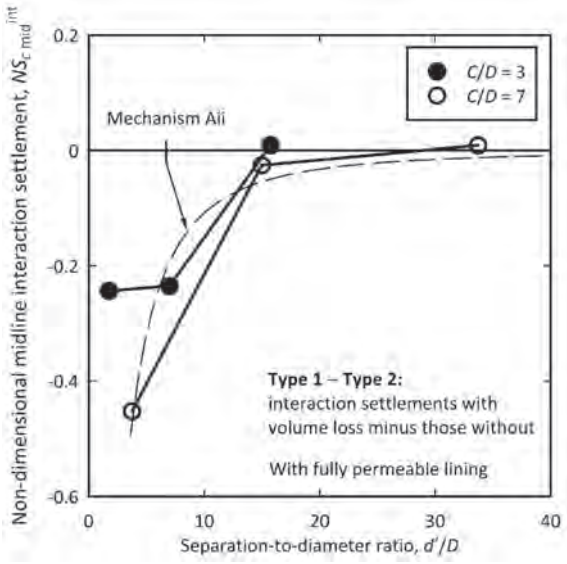


(b) For difference between analyses with and without volume loss

Fig. 8. Variation of maximum normalised interaction surface settlement with tunnel separation.

Laver (2010) pointed out that these theoretical interaction mechanisms are applicable to practical twin-tunnel design. That is, open-face tunnelling usually leads to considerable volume loss as described in Mechanism Ai, whilst pressurized face tunnelling may achieve a near-zero volume loss as considered in Mechanism Aii & Aiii. The relative soil-lining permeability represents different tunnelling conditions; for instance, a permeable lining case (i.e. Mechanisms Ai & Aii) might comprise clayey soil, whereas the

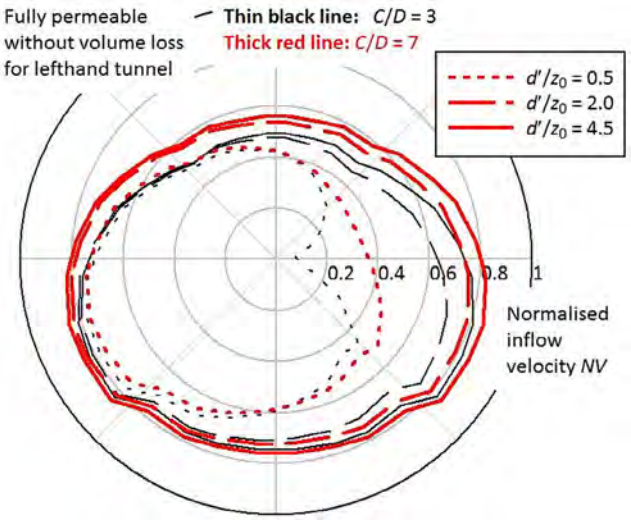


Fig. 9. The inflow velocity distribution around one of the permeable twin-tunnels.

impermeable soil-lining system (i.e. Mechanism Aiii) corresponds to sandy soil as long as the waterproofing of the lining remains effective in the long term. Mechanisms B&C are active at very close tunnel separation, which corresponds to station tunnels with a bigger diameter and small spacing. The proposed consolidation twin-tunnel interaction is complex but cannot be ignored, since it is able to double the horizontal movements and also increase the vertical movement significantly.

However, due to limited computational resources, Laver (2010) only considered three separation-to-depth ratios and two extreme soil-lining permeability conditions for his parametric study. Although the trends for interaction mechanisms were generally identified, predictive equations were not proposed. Further research is required for more numerical parametric study cases along with detailed analytical analyses. If an opportunity occurs in practice, field measurements are highly desirable to compare against the proposed consolidation interaction behaviour.

*Twin tunnel lining behaviour*

Similar to twin-tunnelling induced consolidation ground movements, little research work is found on lining structure behaviour of twin tunnels during consolidation. Wright (2010) points out that the spacing between old twin tunnels in London Underground is normally less than a tunnel diameter (i.e. $d'/D_T < 1$). Such closely-spaced two tunnels may result in a flow field different from a single tunnel. Li et al. (2016) extended the load column analogy proposed by Dimmock (2003) (see Fig. 6b) to explain twin-tunnel interaction during soil consolidation. For closely-spaced twin tunnels, there are three soil columns along the cross-section; one between the two tunnels and two at the other two sides as illustrated in Fig. 10a. If the tunnel lining is permeable relative to the surrounding soil, the middle soil

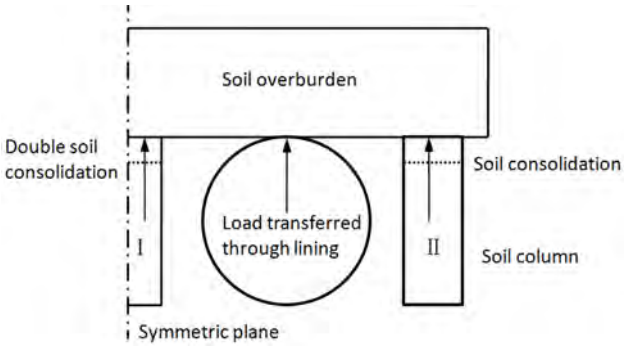


(a) Twin tunnel long-term consoliation load-analogy

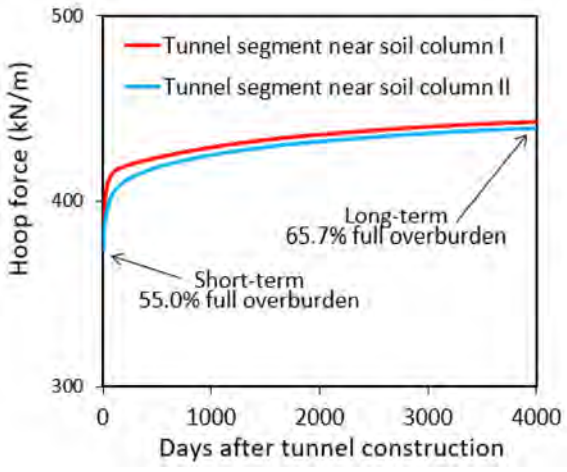


(b) Long-term increase of hoop thrust (Day 0 is the end of tunnel construction)

Fig. 10. Twin tunnel long-term consolidation interaction (Li et al., 2015).

column (see Column I in Fig. 10a) consolidates more rapidly between the twin tunnels than the soil columns at the outer sides (Column II) (i.e. an equivalent shorter drainage path). This differential consolidation condition may cause the rate of soil loading development along the lining to be asymmetric. Fig. 10b shows how the computed hoop thrust forces of tunnel segment in the middle (Soil column I) and tunnel segment at the sides (Soil column II) change over time. As expected, the thrust of the segment in the middle increases at a more rapid rate than that of the segment at the sides due to a shorter drainage path during soil consolidation.

**Cross passage tunnels**

Between two underground tunnels, cross passages are usually constructed as a safe means of egress in case of emergency (PSCG PRC 2004) as illustrated in Fig. 11. The presence of twin tunnels and cross passages alters the original soil arching generated by a single tunnel and add additional drainage paths during consolidation if the lining is permeable. Such effects may change the ground deformation and tunnel structural performance both during excavation and in the long term.

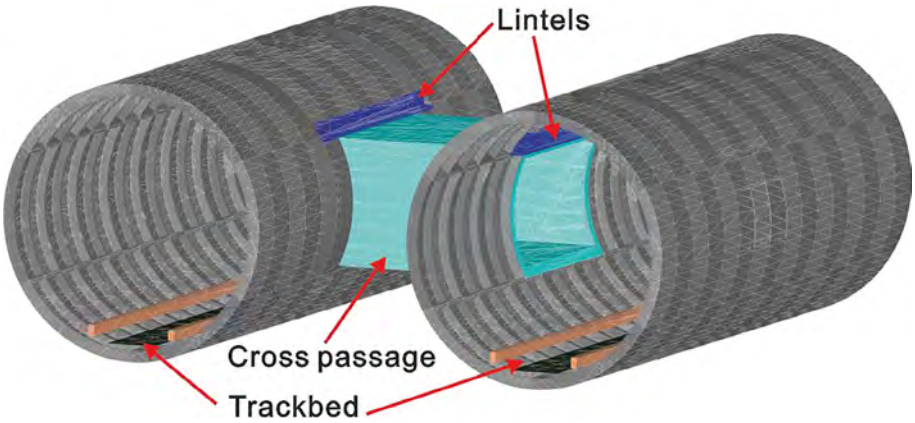


Fig. 11. Illustration of a cross passage (Li et al., 2016).

*Surface movements*

Following the previous effort of single tunnel (Wongsaroj, 2005) and twin tunnels (Laver, 2010), Li et al. (2015) conducted further study to investigate the long-term behaviour of a cross passage between closely-spaced twin tunnels in London clay.

To compare the ground response of twin tunnels with and without a cross passage, Fig. 12a plots the ground surface settlements at the long-term steady state for the two extreme permeability cases: impermeable and fully permeable. There is little difference in the surface settlement profiles of the two cases. Also, the differential settlement along the longitudinal direction is small as shown in Fig. 12b. This indicates, for closely-spaced twin tunnels, the effect of cross passage on surface settlement may not be significant compared to the magnitude of the surface settlement generated by twin tunnel construction. That is, the seepage into twin tunnel dominates the consolidation induced settlement.

Compared to the hydraulic mechanism of a single tunnel, the mechanism of a cross passage with twin tunnels may behave either similar to a small single tunnel (i.e. lower bound) or a big one circumscribing the twin tunnels (i.e. upper bound); the geometries are illustrated in Fig. 13a. Results from finite element simulations compare the pore water pressure profile due to seepage for different tunnel cases as shown in Fig. 13b. It is noted that the pressure contour of the cross passage resembles more like a bigger tunnel than a smaller one, particularly above the tunnel crown.

*Cross passage tunnel behaviour*

The long-term performance of cross passage tunnel sections is often considered to be critical as substantial cracks, serious water infiltration and greatest diametrical distortion are observed therein (e.g. Shen et al., 2014; Wright, 2010). Li et al. (2015) investigated the time-dependent structural behaviour of old cross passage tunnels and highlighted that the performance of the cross passage itself is

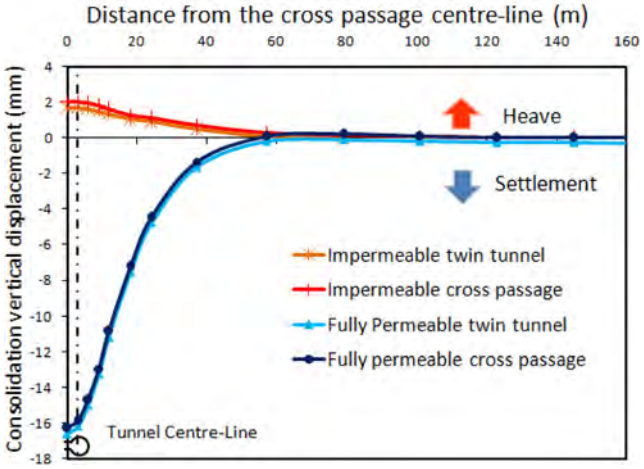


(a) Ground settlement along the transverse settlement trough

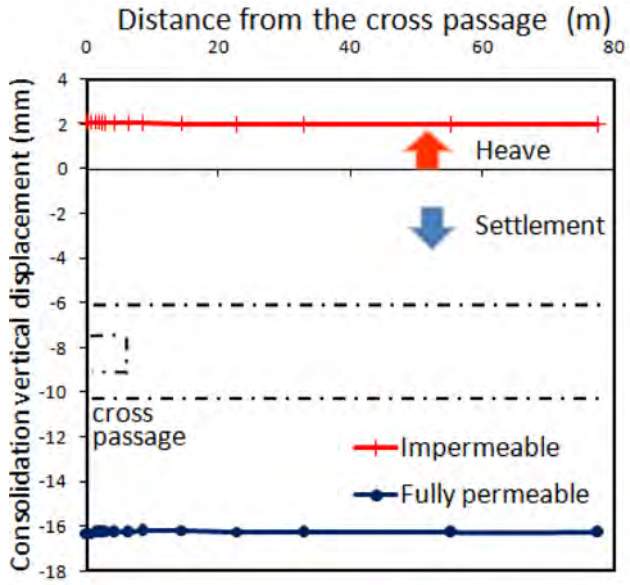


(b) Ground settlement along the longitudinal direction

Fig. 12. Surface settlement at the long-term steady state (short term ground movements are not included) (Li et al., 2015).

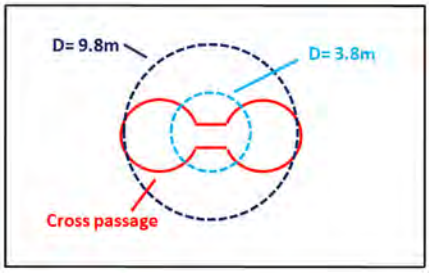


(a) Illustration of the equivalent tunnel diameter

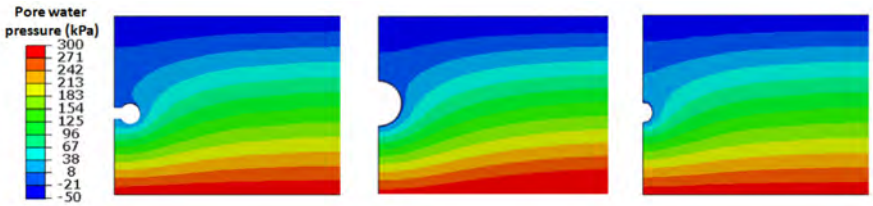


(i) Cross passage (ii) Big tunnel (D=9.8m) (iii) Small tunnel (D=3.8m)

(b) Pore water pressure profile due to seepage into the tunnel

Fig. 13. Ground surface settlement at different relative soil-lining permeability (Li et al., 2015).

very much influenced by the variation in effective stress and pore pressure around the tunnel. In this case, both the twin tunnels and cross passage are assumed as fully permeable since Mair (2008) reports that the measured pore pressure immediately adjacent to old tunnels in low permeability London clay usually is close to zero (i.e. the tunnels act as drains).

The long-term tunnel behaviour of cross passage section is often more structurally critical than the other non-cross passage full ring tunnel sections. At the cross passage section, a lintel may be placed above the tunnel opening (see Fig. 11) to transfer the soil overburden above to the adjacent full rings. Fig. 14 shows the change in tunnel diameter with time along the tunnel rail direction near the cross passage opening section. Compared to the full ring section, the cross passage opening, which is pushed horizontally by soil loading, tends to deform back to the original circular shape due to its stiffness reduction in the horizontal direction (i.e. less tunnel squatting). The change in the vertical diameter at the centre of the cross passage opening (i.e. Ring 0) is 0.94 mm, which is 78.3% of the tunnel diameter change at the full section (i.e. 1.20 mm). The effect of the opening gradually fades out along the rail direction and finally disappears at Ring 12 (i.e. 6.35 metres away from the opening). Along the railway track, the differential tunnel displacement remains localised and the magnitude is very small (i.e. within a few millimetres).

To illustrate the soil arching mechanism above a tunnel opening, a "table" load column model is proposed as shown in Fig. 15a (Li et al., 2015). Similar to the twin tunnel mechanism, the soil overburden is sustained by the tunnel structure together with four "table legs" (i.e. soil load columns) around it considering the symmetry. To focus on the structural response along the lining, Fig. 15b shows the detailed structure of the tunnel cross passage at the X-X cross section, which is a side view of the segmental linings in Fig. 15a. Furthermore, the side view of the cast-iron tunnel segments and the lintel is illustrated at the Y-Y cross section in Fig. 15b. At the right end of the figure, the half-ring above the tunnel opening is numbered as zero, while the other rings are numbered consecutively along the longitudinal railway direction. In accordance with the "table" analogy model, the left-hand side of Ring 0, 1, 2 adjoins to soil column I, while its right-hand side stands for soil column II. Away from the opening, the left-hand side and right-hand side of the rest of the rings are at the position of soil column IV and III, respectively.

Fig. 16a and b shows the hoop thrust at different rings both in the short term and long term, respectively. Of particular interest is the critical Segment B in Ring 3 adjacent to the opening at the axis level. The short term hoop thrust is 128.8% of the overburden, which is significantly higher than the thrust in the non-cross passage section (i.e. 55.0% overburden). After the long term, the thrust continuously builds up to 191.1% of the overburden due to the overburden redistribution as discussed before. This segment is obviously considered to be one of the most critical sections of the cross passage section.

## Closure and recommendations for future study

Tunnels are often used for decades or even longer. This paper describes various mechanisms of long-term ground movements and tunnel behaviour after tunnelling in clayey

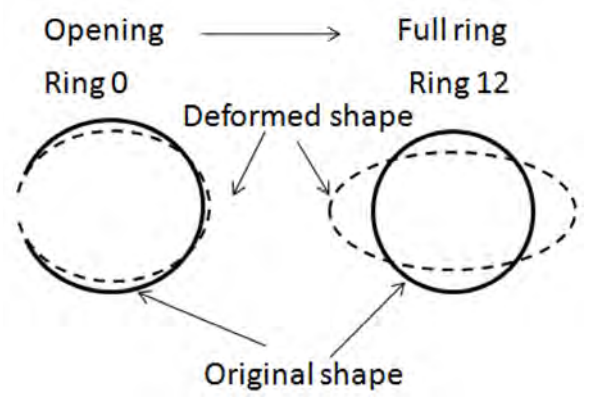


(a) Illustration of tunnel deformation

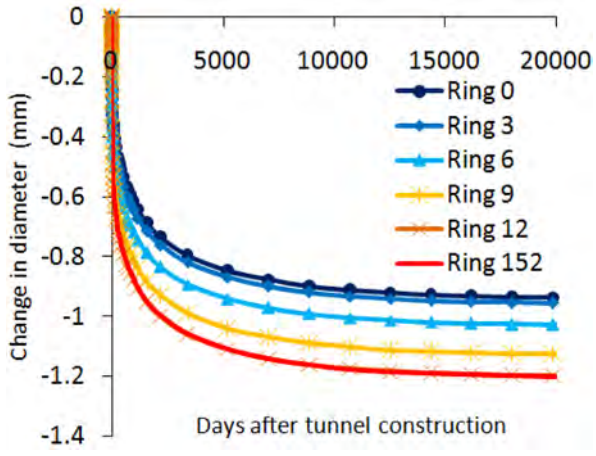


(b) Tunnel vertical deformation

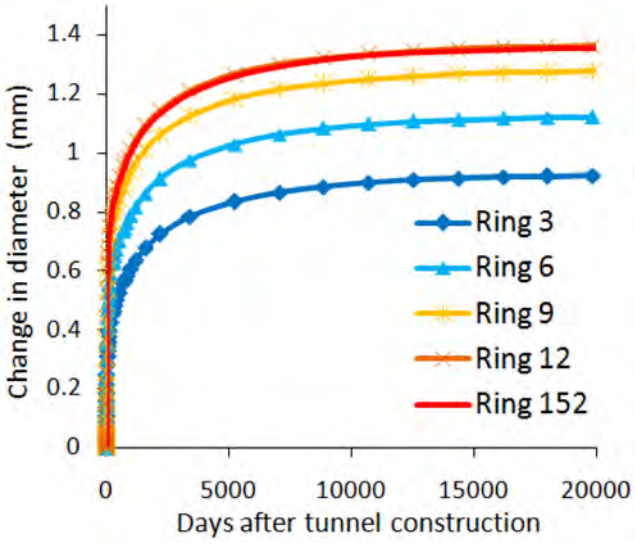


(c) Tunnel horizontal deformation

Fig. 14. Tunnel deformation at different sections along the longitudinal direction (Day 0 is the end of the cross passage tunnel construction) (Li et al., 2015).

soil based on a series of 3D finite element analyses conducted and interpretation of limited field case studies. A single tunnel generates a radial seepage flow around the tunnel during soil consolidation. Twin tunnels and cross passages alter the development of the effective stress and pore pressure around the tunnel with time from the radial seepage condition and therefore complex tunnel-soil interaction occurs. In this paper, the long term behaviour of a single tunnel, twin tunnels and cross passages are discussed with particular emphasis on surface ground movements and tunnel lining behaviour. The main findings that may be of engineering concerns are listed as follows:

1. Ground movements can continue to build up after tunnel construction in clayey soil as the excess pore pressure, which is generated by tunnel excavation, dissipates with time. Also soil consolidation occurs by the new water pressure conditions created by the tunnel that has typically zero pressure inside. If the tunnel is fully permeable, the pore pressure at the soil-tunnel boundary is zero and hence the effective stress in the soil around the tunnel increases with time, causing soil consolidation until the seepage becomes steady state. A seepage rate from low permeability clayey soil is often very small and the groundwater seeping into the tunnel can evaporate quickly. Although a tunnel may look impermeable because the surface is dry, it is possible that the tunnel drainage conditions are fully permeable.
2. A method to evaluate the long-term surface movements above a single tunnel in clayey soil has been proposed. The magnitude of long-term settlements depends on the drainage conditions of the tunnel, the compressibility of the clayey soil and the excess pore pressures generated during tunnel excavation. The conditions of the tunnel to be permeable or impermeable are governed by soil permeability, lining permittivity, tunnel diameter and clay thickness.
3. Horizontal ground strains, which are important in evaluating building damage above tunnels, may continue to increase during soil consolidation up to the similar magnitude to the short-term ground movements induced by tunnel excavation. A method to predict consolidation-induced horizontal strains has been proposed.
4. In both London stiff clay and Shanghai soft soil, metro tunnels usually develop a further squatting after construction as the surrounding ground consolidates. The consolidation time of long-term tunnel deformation is much shorter than that of ground settlement due to difference in times in reaching the quasi-steady state water pressure conditions around and away from the tunnel.
5. Twin-tunnel interaction may increase the long-term ground movements depending on tunnel excavation induced shearing, configuration (spacing-diameter ratio) and relative soil-lining permeability. For side-by-sided twin tunnels, the soil between the closely-space twin

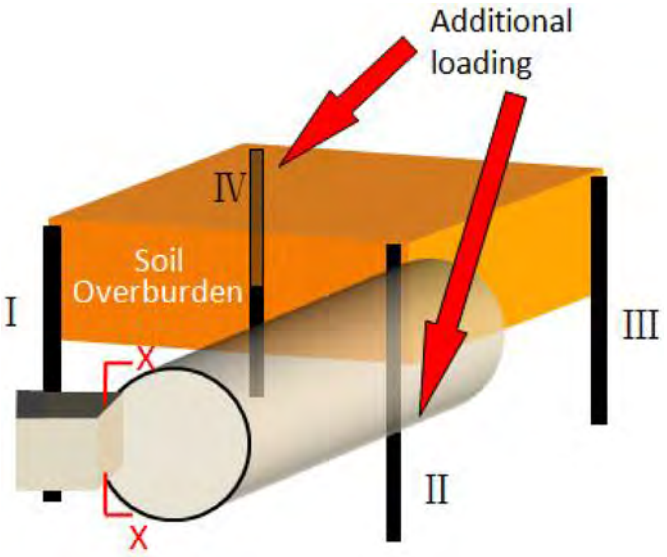


(a) Tunnel load-analogy of a table with four load columns

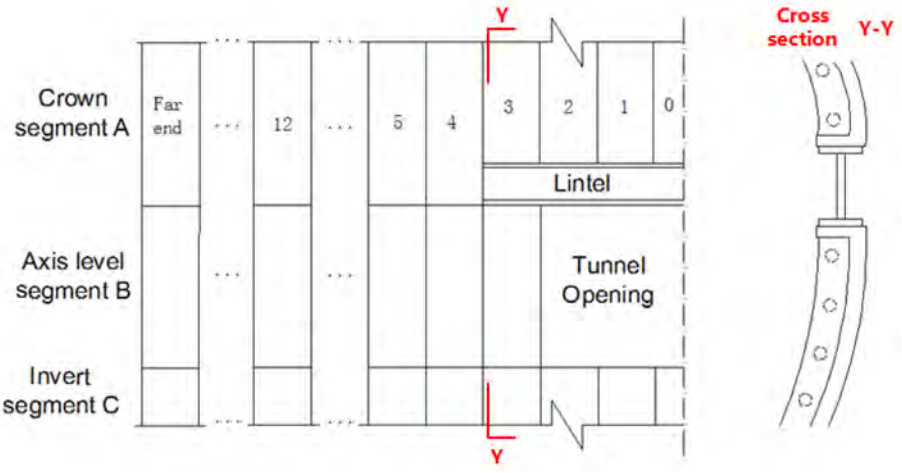


(b) Side view of tunnel opening subjected to soil overburden at cross section X-X

Fig. 15. 3D cross passage tunnel opening (Li et al., 2015).

tunnels consolidates more rapidly than that at the sides, which in turn leads to asymmetric long-term tunnel thrust mode. Such asymmetry may result in uneven railway track movement due to tunnel lining distortion and rotation.

6. In closely-spaced twin tunnels, the presence of cross passage does not appear to increase the magnitude of consolidation induced surface settlement. However, tunnel stress and deformation builds up at the cross passage tunnel opening as the earth pressure redistributes around the structures in the long term.

Most current studies assume the permittivity of tunnel lining as a constant value throughout the whole consolidation process, but omit the change of lining permittivity due to the structure deterioration. Future investigation may evaluate the effect of the changing lining permittivity with time on the soil-tunnel interaction. In addition, current studies on long-term ground movements mainly focus on stiff clays (e.g. London clay), whereas little attention is paid on soft clays (e.g. Shanghai clay) where the magnitude of consolidation-induced ground movements may be more significant than that in stiff clays. Further to the long-term lining and ground movements behaviour of a single tunnel, future research may investigate the long-term consolidation induced soil-tunnel interaction of complex underground structures that exist in urban metro networks of big cities. Of great interest is to acquire more field measurements of the long-term behaviour to further verify the mechanisms presented in this paper.

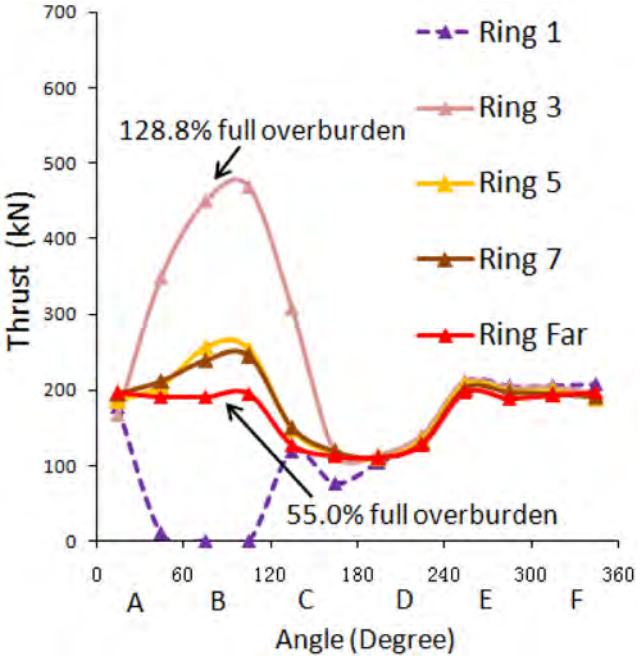


(a) Short term hoop thrust

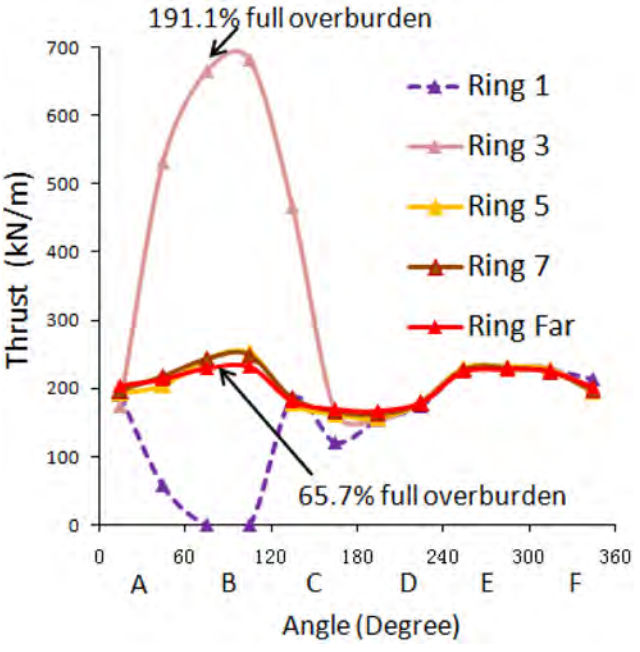


(b) Long term hoop thrust

Fig. 16. Hoop thrust in the tunnel lining for different rings (Li et al., 2015).

## Acknowledgement

This work was supported by National Natural Science Foundation of China (No. 51508403) and by National Natural Science Foundation of China (No. 51608539).

## Appendix A. Evaluation method

In this paper, a brief description of the new evaluation of tunnelling-induced long-term ground movements proposed by Laver et al. (2016) is given as follows:

*Stage 1. Evaluate the dimensionless displacement DS*

In this first step, a dimensionless surface settlement (DS) is adopted to describe the long-term consolidation displacements and strains in response to different lining permeability values. In theory, $DS = 0$ for a fully impermeable lining, and the greater DS is the more permeable lining is relative to surrounding soil up to $DS = 1$ for a fully permeable lining.

*Stage 2. Evaluate steady-state non-dimensional displacement and strain at two limiting cases*

The non-dimensional consolidation-induced maximum displacements and consolidation-induced peak horizontal strains (i.e. maximum compressive horizontal strain at tunnel centreline $\varepsilon_{c\ \max}^{c}$ and maximum tensile horizontal strain in far field, $\varepsilon_{c\ \max}^{f}$) are considered for the two extreme soil-lining permeability cases (subscript *ssp* for fully permeable lining case and subscript *ssi* for impermeable lining case). These non-dimensional parameters depend upon tunnel condition, excavation method, etc., for example cover of soil above tunnel crown over tunnel diameter (cover-to-diameter) $C/D$ ratio, immediate volume loss due to tunnelling $V_L$, and their empirical relationships can be derived as a series of equations from the results of FE simulations.

*Stage 3. Evaluate steady-state non-dimensional displacement and strains at a particular permeability*

To determine the non-dimensional maximum displacements ($NS_{c\ \max(ss)}$ and $NH_{c\ \max(ss)}$) and strains ($\varepsilon_{c\ \max(ss)}^{c}$ $\varepsilon_{c\ \max(ss)}^{f}$) at steady state (ss) conditions for the particular lining and soil permeability conditions considered, $DS$ defined in Stage 1 is used in conjunction with the non-dimensional parameters at the two extreme soil-lining permeability values in Stage 2.

*Stage 4. Convert to actual steady-state displacements and strains*

The computed non-dimensional steady-state displacements are then converted to the actual consolidation-induced vertical and horizontal displacements at steady state conditions.

*Stage 5. Evaluate relative displacement*

The actual ground displacement at any consolidation time of interest is given by scaling the steady-state displacements using a relative displacement $RS_{c\ \max}$, which is related to the dimensionless time factor $T_v$, $C/D$ and $RP$.

*Stage 6. Find the actual consolidation-induced displacements and strains at particular time*

Following Stage 5, the actual maximum consolidation-induced vertical and horizontal displacements and compressive and tensile strains at any consolidation time are calculated from the steady-state maximum displacement and strain scaled by $RS_{c\ \max}$, respectively.

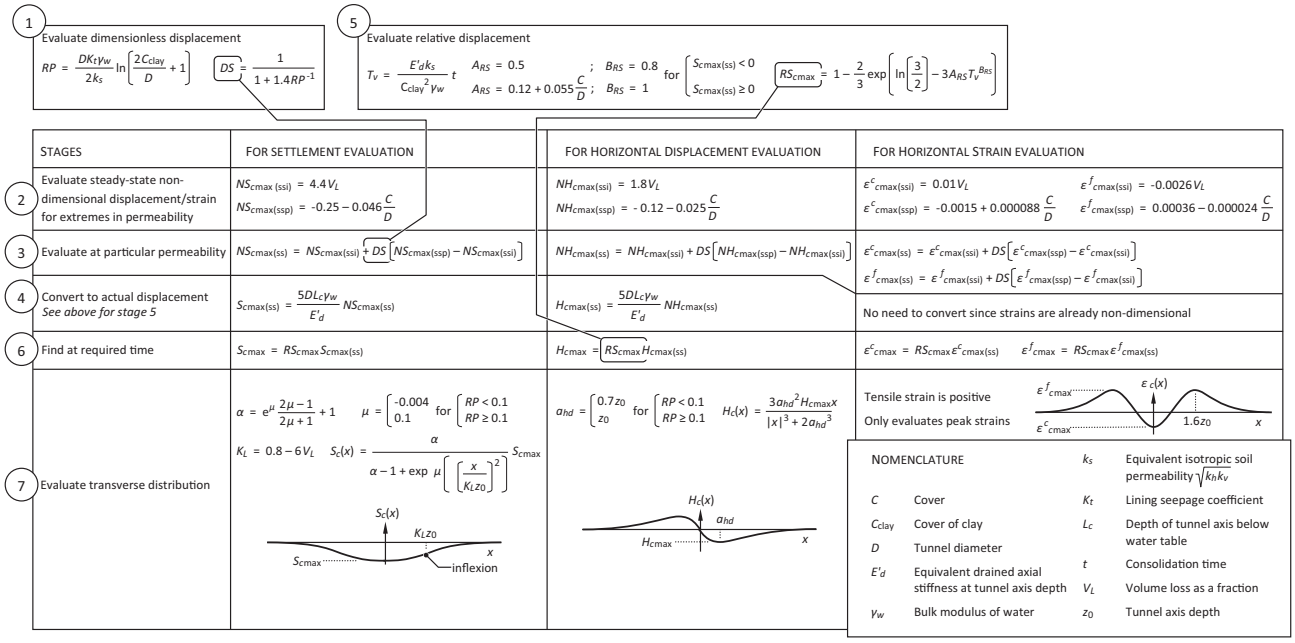


Fig. A1. Outline of the new evaluation method (Laver et al., 2016).

*Stage 7. Evaluate transverse vertical and horizontal displacement distributions*

A modified Gaussian curve suggested by Vorster et al. (2005) is assumed for the settlement trough shape with two extra shape parameters $K_L$ and $\mu$, which enable the modified Gaussian curve to fit the consolidation trough (see Fig. A.1).

Likewise, a two-parameter curve is found to approximate well for the consolidation-induced horizontal displacement distribution. The consolidation-induced horizontal strain distribution is not evaluated since it is usually not a major concern in engineering practice. Instead, the consolidation-induced peak compressive strain $\varepsilon_{c\ \max}^{c}$ at the centreline and the consolidation-induced peak tensile strain $\varepsilon_{c\ \max}^{f}$.

## References


Addenbrooke, T. I. (1996). *Numerical analysis of tunnelling in stiff clay* PhD thesis. Imperial College of Science Technology and Medicine, University of London.

Bowers, K. H., Hiller, D. M., & New, B. M. (1996). Ground movement over three years at the Heathrow Express Trial Tunnel. In *Proceedings of the international symposium on geotechnical aspects of underground construction in soft ground, London* (pp. 557–562).

Burland, J. B. (1995). Assessment of risk of damage to buildings due to tunnelling and excavation. In *Proceedings of the 1st international conference on earthquake geotechnical engineering, IS Tokyo.* .

Dimmock, P. S. (2003). Tunnelling-induced ground and building movement on the Jubilee Line Extension. Ph.D. thesis, University of Cambridge.

Glossop, N. H., & O'Reilly, M. P. (1982). Settlement caused by tunnelling through soft marine silty clay. *Tunnels & Tunnelling, 14*, 13–16.

Harris, D. I. (2002). Long term settlement following tunnelling in overconsolidated London Clay. In *Proceedings of the 3rd international symposium on geotechnical aspects on underground construction on soft ground, Toulouse* (pp. 393–398).

Hover, E., Psomas, S., & Eddie, C. (2015). Short- and long-term tunnelling-induced settlements at Whitechapel Station. *Ground Engineering*, 30–40.

I.T.A. Working Group No. 2. (ITA) (2000). Guidelines for the design of shield tunnel lining. *Tunnelling Underground Space Technology, 15*, 303–331.

Laver, R. (2010). *Long-term Behaviour of twin tunnels in London Clay* Ph. D. thesis. Cambridge, UK: The University of Cambridge.

Laver, R., Li, Z., & Soga, K. (2016). Method to evaluate the long-term surface movements by tunneling in London clay. *Journal of Geotechnical and Geoenvironmental Engineering*. http://dx.doi.org/10.1061/(ASCE)GT.1943-5606.0001611.

Laver, R., Soga, K., Wright, P., & Jefferis, S. (2013). Permeability of aged grout around tunnels in London. *Géotechnique, 63*(8), 651–660.

Lee, K. M., Ji, H. M., Shen, C. K., Liu, J. H., & Bai, T. H. (1999). Ground response to the construction of Shanghai metro tunnel-Line 2. *Soils and Foundations, 39*(3), 113–134.

Li, Z., Soga, K., & Wright, P. (2015). Long-term performance of cast-iron tunnel cross passage in London clay. *Tunnelling and Underground Space Technology, 50*, 152–170.

Li, Z., Soga, K., & Wright, P. (2016). Behaviour of cast-iron cross passage structures and their 3D FE analyses. *Canadian Geotechnical Journal, 53*, 930–945.

Mair, R. J. (2008). Tunnelling and geotechnics: new horizons. *Geotechnique, 58*(9), 695–736.

Martinez, R., Schroeder, F., & Potts, D. (2014). *Long-term settlement following twin tunnel construction*. Santiago, Chile: Viii Congreso Chileno De Ingenieria Geotecnica.

Martos, F. (1958). Concerning an approximate equation of the subsidence trough and its time factors. In *Proceedings of the International Strata Control Congress, Leipzig* (pp. 191–205).

Ng, C. W. W., Liu, G. B., & Li, Q. (2013). Investigation of the long-term tunnel settlement mechanisms of the first metro line in Shanghai. *Canadian Geotechnical Journal, 50*(6), 674–684.

Nyren, R. J. (1998). *Field measurements above twin tunnels in clay* Ph.D. thesis. London: Imperial College of Science, Technology and Medicine.

O'Reilly, M. P., Mair, R. J. & Alderman, G. H. (1991). Long-term settlements over tunnels: an eleven-year study at Grimsby. In *Tunnelling '91* (pp. 55–64). London.

Palmer, J. H. L., & Belshaw, D. J. (1980). Deformations and pore pressure in the vicinity of a precast segmented, concrete-lined tunnel in clay. *Canadian Geotechnical Journal, 17*, 174–184.

Peck, R. B. (1969). Deep excavations and tunnelling in soft ground. In *Proceedings of the 7th international conference on soil mechanics and foundation engineering, Stockholm* (pp. 345–352).

Shen, S., Wu, H., Cui, Y., & Yin, Z. (2014). Long-term settlement behaviour of metro tunnels in the soft deposits of Shanghai. *Tunnelling Underground Space Technology, 40*, 309–323.

Shin, J. H., Potts, D. M., & Zdravkovic, L. (2002). Three-dimensional modelling of NATM tunnelling in decomposed granite soil. *Géotechnique, 52*(3), 187–200.

Shirlaw, J. N. (1995). Observed and calculated pore pressures and deformation induced by earth pressure balance shield. *Canadian Geotechnical Journal, 32*, 181–189.

Terzaghi, K. (1943). *Theoretical soil mechanics*. New York: John Wiley and Sons (pp. 66–76). New York: John Wiley and Sons.

Tube Lines (2007). Deep tube tunnel knowledge & inspection programme Soil Parameters Report, TLL-L001-N416-DTAAWP2-TUN-RPT-00001. London, UK.

Vorster, T. E. B., Klar, A., Soga, K., & Mair, R. J. (2005). Estimating the effect of tunnelling on existing pipelines. *ASCE Journal of Geotechnical and Geoenvironmental Engineering, 131*, 1399–1410.

Wang, Z., Wong, R., Li, S., & Qiao, L. (2012). Finite element analysis of long-term surface settlement above a shallow tunnel in soft ground. *Tunnelling and Underground Space Technology, 30*, 85–92.

Ward, W. H., & Thomas, H. S. H. (1965). The development of earth loading and deformation in tunnel linings in London Clay. *Proceedings of the 6th international conference on soil mechanics and foundations of engineering, Toronto* (Vol. 2, pp. 432–436). .

Wongsaroj, J. (2005). *Three-dimensional finite element analysis of short and long-term ground response to open-face tunnelling in stiff clay* PhD thesis. University of Cambridge.

Wongsaroj, J., Soga, K., & Mair, R. J. (2007). Modelling of long term ground response to tunnelling under St James' Park London. *Geotechnique, 57*, 75–90.

Wongsaroj, J., Soga, K., & Mair, R. J. (2013). Tunnelling-induced consolidation settlements in London Clay. *Geotechnique, 63*, 1103–1115.

Wright, P. (2010). Assessment of London underground tube tunnels – Investigation, monitoring and analysis. *Smart Structures and Systems, 6*, 239–262.

Wu, H., Xu, Y., Shen, S., & Chai, J. (2011). Long-term settlement behavior of ground around shield tunnel due to leakage of water in soft deposit of Shanghai. *Frontiers of Architecture and Civil Engineering in China, 5*(2), 194–198.

Zhang, D., Liu, Y., & Huang, H. (2013). Leakage-induced settlement of ground and shield tunnel in soft clay. *Journal of Tongji University (Natural Science), 41*(8), 1185–1191 (in Chinese).